Characterising carotid atherosclerotic plaques using phantom and computational ultrasound models

to develop a risk stratification tool for cardiovascular disease

clinical research shows

correlation between vulnerable atherosclerotic plaque characteristics and clinical outcomes [12]

biomarkers include

- neovascularisation [5]
- large necrotic core [8]
- thin fibrous cap [6]

need to collect data to

validate with clinical findings [24] [32]

limited by

visualisation in current ultrasound imaging techniques [3][4]

requires

novel ultrasound imaging techniques [29]

using

phantom models

to replicate and validate

Experimental modelling

can be solved by

Goals

needs to

realistic 3D imaging

uses

Field II [25]

simulating

analytical and physiological 2D blood vessel and plaque simulations [28] [41]

simulating

realistic 2D flow field

simulating

use

contain

- parameters
- impulse response [14] [15][16]
- excitation signal

[38]

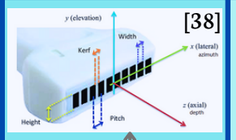

uses

to achieve

adjustable parameters

allow

Accurate simulation of transducer functions

is validated by

simple vessel modelling and steady flow

starting from

Computational modelling

Computational Challenges

such as

flow simulation

uses

- pulsed wave phantom (multi-cpu)[23]
  - *has*
  - calculate psi (Womersly model)
  - parallel processing
- RF-data containing blood and tissue motion [22]
  - *has*
  - velocity profile (Poiseuille's profile) [24]
  - pulsation & respiration movement [25]

uses

- CFD tool box in Matlab [19]
- ANSYS Fluent [20]
- Tecplot [21]

[40]

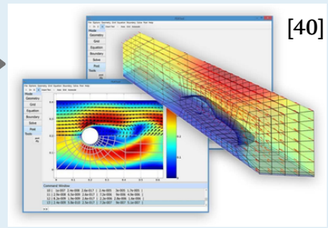

publicly available & expanded dataset

- Carotid Ultrasound Boundary Study (CUBS) [30]
- Cancer Imaging Archive (TCIA) [31]
- Samples generated using Poisson fusion [32]

transfer 2D imaging to 3D [30]

sufficient datasets

are based on

clinical & research datasets

Experimental Challenges

must be

- durable and reusable [26]
- *must include*
  - an embedded plaque with micro vasculature [36]
- *require*
  - accurate mechanical and acoustic properties

achieved by selecting

suitable materials

to model the atherosclerotic vessel

[39]

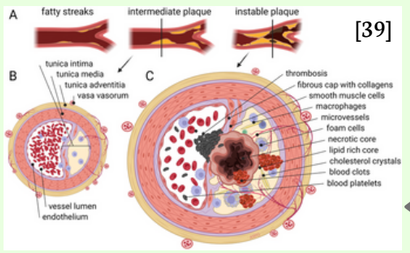

such as

- PVA [1]
  - *exhibits*
  - accurate elastic, flexible, and acoustic properties [34]
    - *and is*
    - suitable for long-term
      - *can simulate*
      - artery
  - *follows these procedures*
  - dissolution
  - freeze-thaw crosslinking [35]
  - demolding and rinsing
- PVA-based hydrogel
  - *can mimic*
  - Tissues with different echogenic characteristics
    - *can simulate*
    - intima + fibrous cap
  - *by adding various material*
  - *follows these procedures*
  - dissolution
  - addition [2]
  - crosslinking treatment
  - 3D printed mold [27]
  - rinsing
- Silica Gel [33]
  - *if it is of low density*
  - Hypoechoic and weakly reflective layer
    - *can simulate*
    - plaque core layer
  - *follows these procedures*
  - precursor preparation
  - Base catalysis
  - Hypoechoic and weakly reflective layer
  - 3D printed mold [27]
  - Supercritical drying

these can be bonded together by hot melt bonding

Experimental Solutions

hot melt bonding between two layers

follows these procedures

- control heat application
- quick bonding and cooling
- edge pressure
- reduced interference

Computational Solutions

- B-mode [17][18]
  - *simulates*
  - mechanical scanning
    - *aligns*
    - echo lines to a common start time
      - *plot*
      - grayscale image (dB scale)
- A-mode
  - *defines*
  - position and scattering amplitude of targets
    - *calculate*
    - echos from targets
      - *compute*
      - envelop (Hilbert transform)
        - *plots*
        - amplitude image

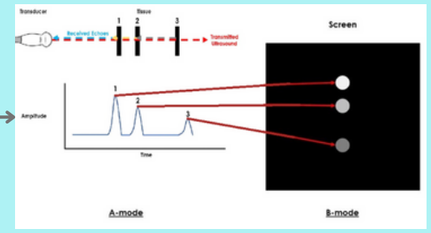

[37]

References :

[1] Kumar, A. and Han, S.S. (2016) 'PVA-based hydrogels for tissue engineering: A review', *Journal of Macromolecular Science, Part A*, 53(3), pp. 159–182. DOI: 10.1080/00914037.2016.1190930.

[2] Huang, M., Hou, Y., Li, Y., Wang, D. and Zhang, L. (2017) 'High performances of dual network PVA hydrogel modified by PVP using borax as the structure-forming accelerator', *Designed Monomers and Polymers*, 20(1), pp. 505–513.

[3] Kumar, A. and Han, S.S. (2021) 'Carotid Atherosclerosis, Ultrasound and Lipoproteins', *Biomedicines*, 9(5), p. 521.

[4] Virmani, R., Burke, A.P., Farb, A. and Kolodgie, F.D. (2011) 'Pathology of the vulnerable plaque', *Journal of the American College of Cardiology*, 57(20), pp. 2031–2042. DOI: 10.1016/j.jacc.2011.02.018.

[5] Lu, X., Zhao, Y., Sun, Y., Jin, Z. and Xin, Y. (2015) 'Vasa Vasorum in Atherosclerosis and Clinical Significance', *International Journal of Molecular Sciences*, 16(5), pp. 11574–11608.

[6] Redgrave, J.N., Gallagher, P., Lovett, J.K. and Rothwell, P.M. (2008) 'Critical cap thickness and rupture in symptomatic carotid plaques: the Oxford Plaque Study', *Stroke*, 39(6), pp. 1722–1729. DOI: 10.1161/STROKEAHA.107.507988.

[7] Seekircher, L., Tschiderer, L. and Willeit, P. (2024) 'Intima-media thickness at the near or far wall of the common carotid artery in cardiovascular risk assessment', *European Heart Journal Open*, 3(5), oead089.

[8] Redgrave, J.N., Lovett, J.K., Gallagher, P.J. and Rothwell, P.M. (2006) 'Histological assessment of 526 symptomatic carotid plaques in relation to the nature and timing of ischemic symptoms: the Oxford Plaque Study', *Circulation*, 113(19), pp. 2320–2328.

[9] Kumar, A. and Han, S.S. (2021) 'A review of carotid artery phantoms for Doppler ultrasound imaging', *Journal of Medical Ultrasound Technology*, 29(3), pp. 159–182.

[10] Kamenskiy, A.V., MacTaggart, J.N., Pipinos, I.I., Bikhchandani, J. and Dzenis, Y.A. (2012) 'Three-dimensional geometry of the human carotid artery', *Journal of Biomechanical Engineering*, 134(6), p. 064502.

[11] Zamani, M., Skagen, K., Scott, H., Russell, D. and Skjelland, M. (2020) 'Advanced ultrasound methods in assessment of carotid plaque instability: A prospective multimodal study', *BMC Neurology*, 20(1), p. 39.

[12] Harsham, S.K., Lu, S. and Aggarwal, N. (2018) 'Imaging of atherosclerotic plaque: Correlation of plaque morphology with clinical outcomes', *American Journal of Neuroradiology*, 39(2), pp. E9–E10.

[13] Jensen, J.A. (1996) 'Field: A program for simulating ultrasound systems'. Paper presented at the 10th Nordic-Baltic Conference on Biomedical Imaging, *Medical & Biological Engineering & Computing*, 34(Supplement 1), pp. 351–353.

[14] Tupholme, G.E. (1969) 'Generation of acoustic pulses by baffled plane pistons', *Mathematika*, 16, pp. 209–224.

[15] Stepanishen, P.R. (1971a) 'The time-dependent force and radiation impedance on a piston in a rigid infinite planar baffle', *Journal of the Acoustical Society of America*, 49(3), pp. 841–849.

[16] Stepanishen, P.R. (1971b) 'Transient radiation from pistons in an infinite planar baffle', *Journal of the Acoustical Society of America*, 49, pp. 1627–1638.

[17] Jensen, J.A. and Munk, P. (1997) 'Computer phantoms for simulating ultrasound B-mode and CFM images', *Acoustical Imaging*, 23, pp. 75–80.

[18] Stoitsis, J., Golemati, S., Koropouli, V. and Nikita, K.S. (2008) 'Simulating dynamic B-mode ultrasound image data of the common carotid artery'. *IEEE International Workshop on Imaging Systems and Techniques – IST 2008*, Chania, Greece, 10–12 September 2008, pp. 1–6. DOI: 10.1109/IST.2008.4659999.

[19] MathWorks (2024) *CFDTool - MATLAB, OpenFOAM, and CFD Fluid Dynamics Toolbox*. Available at: https://uk.mathworks.com/matlabcentral/fileexchange/72640-cfdtool-matlab-openfoam-and-cfd-fluid-dynamics-toolbox (Accessed: 20 November 2024).

[20] ANSYS (2024) *Ansys Fluent*. Available at: https://www.ansys.com/products/fluids/ansys-fluent (Accessed: 20 November 2024).

[21] Tecplot (2024) *FieldView: CFD Post-Processing Software*. Available at: https://tecplot.com/products/fieldview/ (Accessed: 20 November 2024).

[22] Field II (2024) 'Tissue Motion Example'. Available at: https://field-ii.dk/?examples/tissue_motion/tissue_motion.html (Accessed: 20 November 2024).

[23] Field II (2024) 'Flow Example'. Available at: https://field-ii.dk/?examples/flow_example/flow_example.html (Accessed: 20 November 2024).

[24] Hoskins, P.R. (2008) 'Simulation and validation of arterial ultrasound imaging and blood flow', *Ultrasound in Medicine & Biology*, 34(5), pp. 693–717.

[25] Jensen, J.A. (2004) 'Simulation of advanced ultrasound systems using Field II'. *Biomedical Imaging: Macro to Nano, IEEE International Symposium on*, pp. 636–639.

[26] Boekhoven, R.W., Rutten, M.C.M., van de Vosse, F.N. and Lopata, R.G.P. (2014) 'Design of a fatty plaque phantom for validation of strain imaging'. *2014 IEEE International Ultrasonics Symposium Proceedings*, pp. 2619–2622. DOI: 10.1109/ULTSYM.2014.0654.

[27] Galluzzo, F., Leonardo, F., Ceruti, A., De Marchi, L. and Corsi, C. (2015) 'Design of anthropomorphic atherosclerotic carotid artery flow phantoms for ultrasound images', *Computing in Cardiology 2015*, 42, pp. 721–724.

[28] Balocco, S., Basset, O., Azencot, J., Tortoli, P., and Cachard, C., (2008) '3D dynamic model of healthy and pathologic arteries for ultrasound technique evaluation'. *Medical Physics*, vol. 35, no. 12, pp. 5440-5450. DOI: 10.1118/1.3006948.

[29] Feinstein, S.B. (2006) 'Contrast ultrasound imaging of the carotid artery vasa vasorum and atherosclerotic plaque neovascularization', *Journal of the American College of Cardiology*, 48(2), pp. 236–243. DOI: 10.1016/j.jacc.2006.02.068.

[30] Lee, K.W., Wood, N.B. and Xu, X.Y. (2004) 'Ultrasound image-based computer model of a common carotid artery with a plaque', *Medical Engineering & Physics*, 26(10), pp. 823–840.

[31] Meiburger, K.M., Zahnd, G., Faita, F., Loizou, C.P., Carvalho, C., Steinman, D.A., Gibello, L., Bruno, R.M., Marzola, F., Clarenbach, R., Francesconi, M., Nicolaides, A.N., Campilho, A., Ghotbi, R., Kyriacou, E., Navab, N., Griffin, M., Panayiotou, A.G., Gherardini, R., Varetto, G. and Molinari, F. (2021) 'Carotid Ultrasound Boundary Study (CUBS): An open multicenter analysis of computerized intima–media thickness measurement systems and their clinical impact', *Ultrasound in Medicine & Biology*, 47(8), pp. 2442–2455.

[32] Li, Y., Li, W., Li, Q., Gao, L., Wang, Y., Li, S. and Wu, B. (2024) 'Research on carotid artery plaque anomaly detection algorithm based on ultrasound images', *Computers in Biology and Medicine*, 182, p. 109180.

[33] Easton, M. (1994) 'The sol-gel preparation of silica gels', *Journal of Chemical Education*, 71(7), p. 599.

[34] Gupta, S., Goswami, S. and Sinha, A. (2012) 'A combined effect of freeze-thaw cycles and polymer concentration on the structure and mechanical properties of transparent PVA gels', *Biomedical Materials*, 7(1), p. 015006.

[35] Henriques, J., Amaro, A.M. and Piedade, A.P. (2024) 'Biomimicking atherosclerotic vessels: A relevant and (yet) sub-explored topic', *Biomimetics*, 9(3), p. 135. DOI: 10.3390/biomimetics9030135.

[36] Adusei, S., Ternifi, R., Fatemi, M. and Alizad, A. (2023) 'Custom-made flow phantoms for quantitative ultrasound microvessel imaging', *Ultrasonics*, 134, p. 107092. DOI: 10.1016/j.ultras.2023.107092.

[37] IMV Imaging (2023) *The A, B, M's: Ultrasound modes explained*. Figures 1 and 2. Available at: https://www.imv-imaging.com/en/2023/04/news-the-a-b-ms-ultrasound-modes-explained/

[38] A mode and B mode imaging, *Detailed explanation of ultrasound image mode A, B, and M*. Figure 1. Available at: https://blog.csdn.net/weixin_38452364/article/details/116657840

[39] Dudley, A.C. and Griffioen, A.W. (2023) 'Pathological angiogenesis: mechanisms and therapeutic strategies', *Angiogenesis*, 26(3), pp. 313–347. DOI: 10.1007/s10456-023-09876-7.

[40] CFD tool box in Matlab diagram, FEATool Multiphysics, Available at: https://www.featool.com/news/2016/07/05/FEATool-v1p5-Released/

[41] Hu, X., Zhang, Y., Gao, L., Cai, G., Jia, Z., Zhang, K. and Deng, L. (2015) 'An ultrasound simulation method for carotid arteries with a wall structure of three membranes', *Acta Acustica*, 40(6), pp. 872–877.